

Indirect Microwave Holographic Imaging of Concealed Ordnance for Airport Security Imaging Systems

Okan Yurduseven^{1, 2, *}

Abstract—In this paper, indirect microwave holographic imaging of concealed ordnance is demonstrated. The proposed imaging technique differs from conventional microwave imaging methods in that it does not require the direct measurement of the complex field scattered from the imaged object but mathematically recovers it from intensity-only scalar microwave measurements. This brings the advantages of simplifying the hardware implementation and significantly reducing the cost of the imaging system. In order to demonstrate the ability of the proposed technique to reconstruct good quality images of concealed ordnance, indirect microwave holographic imaging of a metallic gun concealed in a pouch is carried out for airport security imaging applications. It is demonstrated that good resolution amplitude and phase images of concealed objects can be recovered when back-propagation is applied.

1. INTRODUCTION

The use of microwaves and millimeter-waves for the imaging of concealed objects in security applications is of great importance due to their ability to penetrate through optically opaque materials. In view of this, a significant amount of research, which is mostly based upon direct holography [1, 2], inverse scattering [3–5], synthetic aperture radar (SAR) [6], inverse SAR (ISAR) [7] and microwave tomography [8–11] imaging techniques, has been performed in this field with promising results. However, a major disadvantage associated to these conventional imaging techniques is the requirement of using expensive vector measurement equipment in order to measure the complex field scattered from the imaged object.

Indirect microwave holographic imaging differs from conventional microwave imaging techniques in that it does not require the use of expensive vector measurement equipment to obtain the complex field scattered from the object under imaging, but mathematically recovers it from low-cost intensity-only scalar microwave measurements. This simplifies the hardware implementation and significantly reduces the cost of the imaging system.

In this paper, the use of indirect microwave holography for the phaseless imaging of concealed ordnance is demonstrated. In the literature, indirect microwave holography was proved to have a significant potential to be employed in the measurement of complex antenna near-field and far-field radiation patterns [12, 13]. Recently, this technique has been extended to the imaging of early-stage breast cancer tumors [14] and unconcealed metallic objects [15]. Although promising results have been achieved in [14, 15], the reconstruction of the original scattered field in these works was limited to the measurement plane. This brings a significant challenge for the imaging of concealed objects, which requires the reconstruction of the scattered field at the object plane under the concealed medium to achieve optimum imaging response. In this paper, this challenge is addressed by back-propagating the reconstructed original scattered field at the measurement plane to the plane of the concealed object and it is demonstrated that good quality images of concealed objects can be achieved when the back-propagation algorithm is applied.

Received 23 March 2014, Accepted 8 April 2014, Scheduled 14 April 2014

* Corresponding author: Okan Yurduseven (okanyurduseven@ieee.org).

¹ Center for Metamaterials and Integrated Plasmonics, Duke University, Durham, NC 27708, United States. ² Faculty of Engineering and Environment, Northumbria University, NE1 8ST, United Kingdom.

2. INDIRECT MICROWAVE HOLOGRAPHIC IMAGING

A diagrammatic representation of the indirect microwave holographic imaging system is demonstrated in Figure 1(a) while the imaging system set-up is shown in Figure 1(b).

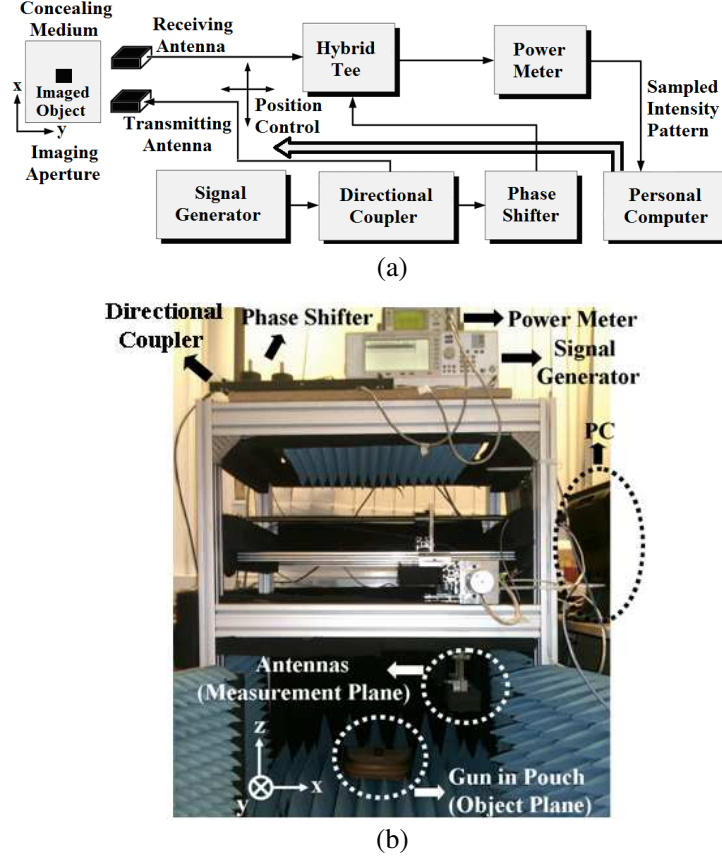


Figure 1. Indirect microwave holographic imaging system, (a) diagrammatic representation, (b) imaging system set-up for the imaging of concealed ordnance.

As can be seen in Figure 1, the indirect microwave holographic imaging system consists of two computer controlled open-ended waveguide antennas performing a point-by-point scan across the imaging plane (x - y plane) with a sample spacing of Δx and Δy in the x - and y -axes. The waveguide antennas have an operational cut-off frequency range of 7.5–12.5 GHz. While one waveguide antenna acts as a transmitting antenna, the other acts as a receiving antenna. The transmitting antenna is fed through an RF signal generator and radiates towards the imaged object at each sampling point. The receiving antenna collects the scattered signal from the object at the corresponding sampling point and feeds it to a hybrid tee where the scattered signal is combined with a reference signal which is tapped from the RF signal generator through a directional coupler. The obtained data at the output of the scalar microwave power meter, $I(x, y)$, can be given as

$$I(x, y) = |E_s(x, y) + E_r(x, y)|^2 \quad (1)$$

Equation (1) denotes the holographic intensity pattern of the imaged object, in which $E_s(x, y)$ is the scattered field from the object while $E_r(x, y)$ is the introduced coherent reference signal. From Equation (1) the following can be obtained

$$I(x, y) = |E_s(x, y)|^2 + |E_r(x, y)|^2 + E_s^*(x, y)E_r(x, y) + E_s(x, y)E_r^*(x, y) \quad (2)$$

As can be seen in Equation (2), while the first and second components are amplitude only components, the third and fourth components have a complex form and therefore consist of amplitude and phase

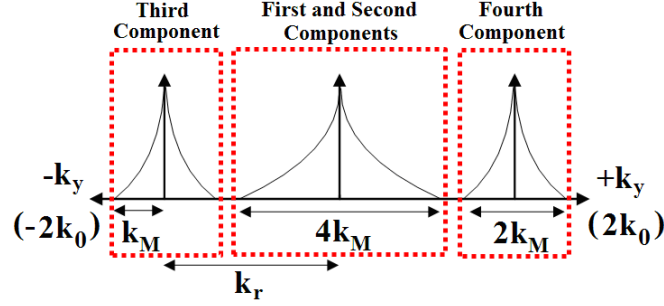


Figure 2. PWS of the object under imaging when the reference signal linear phase shift is applied in the y -axis.

data. Both of these components contain the required complex field scattered from the imaged object. Fourier transform of Equation (2) gives the following

$$F \{I(x, y)\} = F \left\{ |E_s(x, y)|^2 \right\} + F \left\{ |E_r(x, y)|^2 \right\} + F \{E_s^*(x, y)\} \otimes F \{E_r(x, y)\} + F \{E_s(x, y)\} \otimes F \{E_r^*(x, y)\} \quad (3)$$

Equation (3) is known as the plane wave spectrum (PWS) of the imaged object, which is illustrated in Figure 2.

As shown in Figure 2, while the sum of the first and second components in Equation (3) are placed in the center of the spectrum due to their scalar-only DC structure, the third and fourth components are shifted towards the edges of the PWS due to the convolution of the scattered field with the introduced coherent reference signal in the frequency domain. In Figure 2, k_r is the offset wave vector introduced by the reference signal which can be given as

$$E_r = \begin{cases} E_0 e^{-ik_r x}, & x\text{-axis phase shift} \\ E_0 e^{-ik_r y}, & y\text{-axis phase shift} \end{cases} \quad (4)$$

where,

$$k_r = \begin{cases} \Delta\phi/\Delta x, & x\text{-axis phase shift} \\ \Delta\phi/\Delta y, & y\text{-axis phase shift} \end{cases} \quad (5)$$

In Equation (5), $\Delta\phi$ denotes the linear phase shift introduced by the coherent reference signal and can be applied in the x -axis, in the y -axis or as a combination of both.

Given that the PWS of the imaged object is band limited to $\pm k_M$ as can be seen in Figure 2, k_r should be selected as $k_r \geq 3k_M$ to ensure that no overlap is present in the PWS to achieve a correct filtering of the PWS components. In this paper, $\Delta\phi$ is applied in the y -axis and selected as $2\pi/3$ rad. while sample spacing Δx and Δy is selected as $\lambda_0/4$ resulting in a separation of $k_r = 4k_0/3$ between the PWS components in Figure 2, where k_0 is the wavenumber in free space. Introducing the offset wave vector in this manner enables the offset wave vector to exceed k_0 and extend into the invisible region as demonstrated in Figure 2.

As both the third and fourth components in Figure 2 contain the required scattered field data, selecting one of these components is sufficient in order to reconstruct the original scattered field. In this paper, the fourth component in Equation (3) is selected and filtered as follows

$$F' \{I(x, y)\} = F \{E_s(x, y)\} \otimes F \{E_r^*(x, y)\} \quad (6)$$

Taking the inverse Fourier transform of Equation (6) provides the original scattered field from the object under imaging at the measurement plane, $z = 0$,

$$E(x, y, z = 0) = |E_r|^2 E_s(x, y) \quad (7)$$

While the magnitude of the recovered complex scattered field in Equation (7), $|E(x, y, z = 0)|$, produces the reconstructed amplitude image of the imaged object at the measurement plane, $z = 0$, the angle data, $\angle E(x, y, z = 0)$, provide the reconstructed phase image. In order to obtain the complex scattered

field at the object plane at a distance of $z = d$ from the measurement plane, $z = 0$, back-propagation is applied following the definition of the wave propagation vector in the propagation axis (z -axis), k_z , as a function of wave propagation vectors in the x - and y -axes, k_x and k_y , as follows

$$k_z = \begin{cases} \sqrt{k_0^2 - k_x^2 - k_y^2}, & k_0^2 \geq k_x^2 + k_y^2 \\ -i\sqrt{k_x^2 + k_y^2 - k_0^2}, & k_0^2 < k_x^2 + k_y^2 \end{cases} \quad (8)$$

Introducing k_z enables the filtered fourth PWS component at the measurement plane, $z = 0$, given in Equation (6) to be back-propagated to the object plane, $z = d$, whose inverse Fourier transform gives the complex scattered field at the plane of the imaged object, $E(x, y, z = d)$,

$$E(x, y, z = d) = F^{-1} \left\{ F' \{ I(x, y) \} e^{-ik_z d} \right\} \quad (9)$$

While the amplitude of the obtained field in Equation (9), $|E(x, y, z = d)|$, produces the reconstructed back-propagated amplitude image, the phase data, $\angle E(x, y, z = d)$, provide the back-propagated phase image of the imaged object.

3. IMAGING RESULTS AND DISCUSSIONS

In order to demonstrate the ability of the proposed indirect microwave holographic imaging technique with back-propagation to produce good quality images of concealed ordnance, the imaging of a printed



Figure 3. Imaged metallic gun concealed in a pouch.

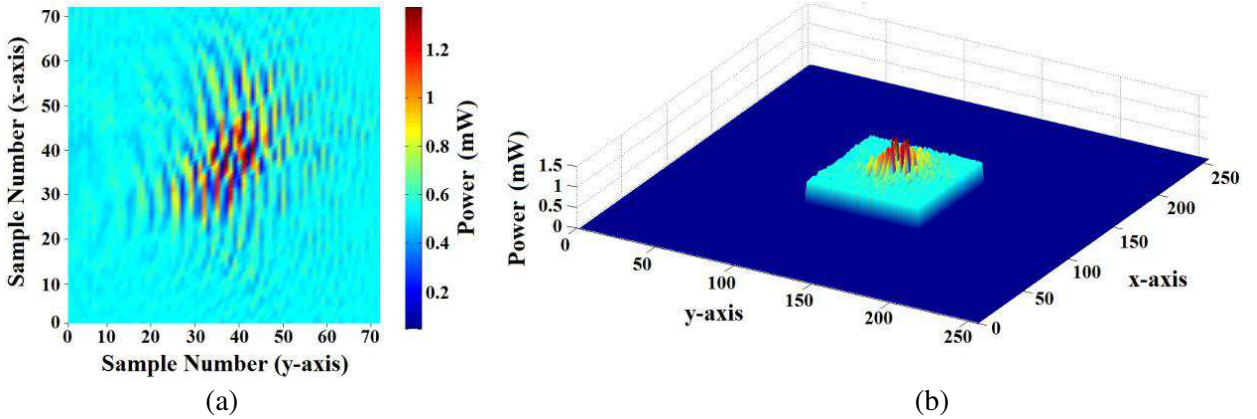


Figure 4. Holographic intensity pattern of the concealed gun, (a) original 72×72 matrix, (b) zero padded 256×256 matrix.

metallic gun concealed in a pouch was carried out. The indirect microwave holographic imaging measurement set-up of the metallic gun concealed in the pouch is demonstrated in Figure 3.

As can be seen in Figure 3, the gun was printed upon a piece of cardboard and placed inside the pouch at a distance of $z = 200$ mm from the antennas in the measurement plane, $z = 0$. The measurements were taken at 12.5 GHz over an imaging aperture of $432 \text{ mm} \times 432 \text{ mm}$ with a sample spacing of $\Delta x = \Delta y = 6 \text{ mm}$ in the x - and y -axes, $\lambda_0/4$, producing a square holographic intensity pattern matrix consisting of 72×72 elements as demonstrated in Figure 4(a). The obtained holographic intensity pattern matrix was then zero padded to 256×256 as shown in Figure 4(b) to smooth the Fourier transform response and Fourier transformed in order to obtain the PWS of the gun as demonstrated in Figure 5.

The fourth component highlighted in Figure 5 was selected and inverse Fourier transformed to recover the complex scattered field at the measurement plane while the DC first and second central components and the third component were filtered off. The reconstructed amplitude and phase images at the measurement plane are shown in Figure 6 with the actual position and outline of the gun in the pouch highlighted.

As can be seen in Figure 6(a), although the reconstructed amplitude image at the measurement plane reveals the presence of an object concealed in the pouch, it is rather difficult to discern the original outline of the gun from this image. The reconstructed phase image at the measurement plane in Figure 6(b), on the other hand, provides only an approximate outline of the concealed gun. From Figure 6, it is evident that improvement is required in order to achieve sufficient information for the identification of the imaged gun in the pouch. To this end, the reconstructed scattered field at the measurement plane, $z = 0$, was back-propagated to the plane of the concealed gun, $z = 200$ mm, and the amplitude and phase images were recovered as illustrated in Figure 7.

As can be seen in Figure 7(a), the reconstructed back-propagated amplitude image at the object plane provides excellent agreement with the actual position and outline of the concealed gun in the

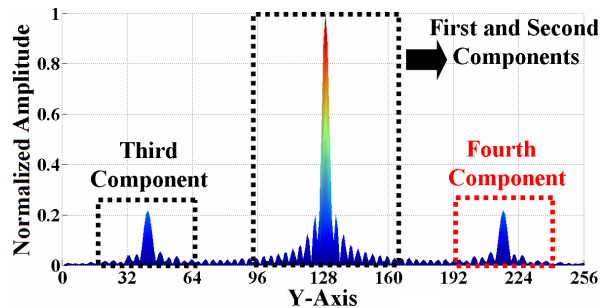


Figure 5. PWS of the imaged metallic gun concealed in the pouch.

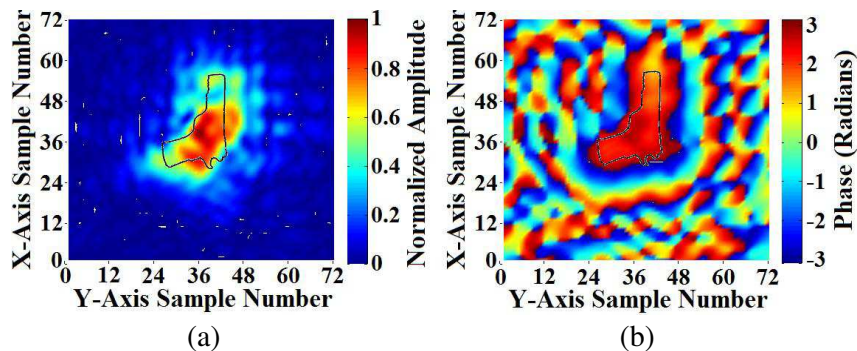


Figure 6. Reconstructed images of the concealed gun in the pouch — measurement plane, $z = 0$, (a) reconstructed amplitude image, (b) reconstructed phase image.

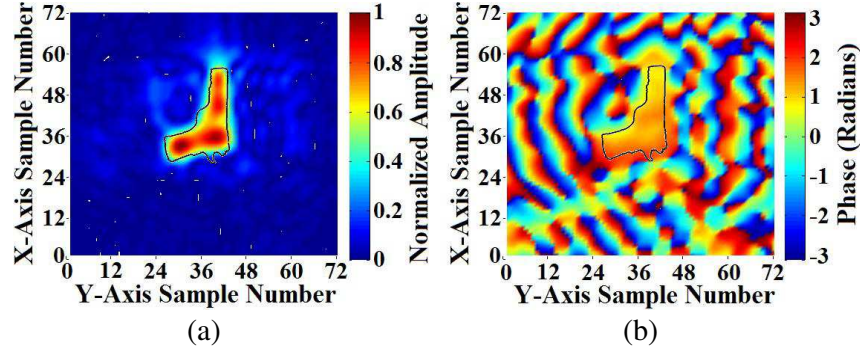


Figure 7. Reconstructed back-propagated images of the concealed gun in the pouch — object plane, $z = 200$ mm, (a) reconstructed amplitude image, (b) reconstructed phase image.

pouch. Similarly, the back-propagated reconstructed phase image in Figure 7(b) is in good agreement with the original extent of the gun, significantly assisting the identification of the imaged gun concealed in the pouch.

4. CONCLUSION

The indirect microwave holographic imaging of a metallic gun concealed in a pouch has been demonstrated. It has been shown that the proposed indirect microwave holographic imaging technique can mathematically recover the complex field scattered from the imaged object using low-cost intensity-only scalar microwave measurements and produces good quality images when back-propagation is applied. The proposed method has a significant potential to be employed in a wide range of imaging applications, including cost-effective security imaging of concealed ordnance in passenger bags at airports.

REFERENCES

1. Sheen, D. M., D. L. McMakin, and T. E. Hall, “Three-dimensional millimeter-wave imaging for concealed weapon detection,” *IEEE Transactions on Microwave Theory and Techniques*, Vol. 49, No. 9, 1581–1592, September 2001.
2. Ren, B., S. Li, H.-J. Sun, W. Hu, and X. Lv, “Modified cylindrical holographic algorithm for three-dimensional millimeter-wave imaging,” *Progress In Electromagnetics Research*, Vol. 128, 519–537, 2012.
3. Shea, J. D., B. D. van Veen, and S. C. Hagness, “A TSVD analysis of microwave inverse scattering for breast imaging,” *IEEE Transactions on Biomedical Engineering*, Vol. 59, No. 4, 936–945, April 2012.
4. Chen, X., K.-M. Huang, and X.-B. Xu, “Microwave imaging of buried inhomogeneous objects using parallel genetic algorithm combined with FDTD method,” *Progress In Electromagnetics Research*, Vol. 53, 283–298, 2005.
5. Catapano, I. and L. Crocco, “A qualitative inverse scattering method for through-the-wall imaging,” *IEEE Geoscience and Remote Sensing Letters*, Vol. 7, No. 4, 685–689, October 2010.
6. Martinez-Lorenzo, J. A., F. Quivira, and C. M. Rappaport, “SAR imaging of suicide bombers wearing concealed explosive threats,” *Progress In Electromagnetics Research*, Vol. 125, 255–272, 2012.
7. Demirci, S., H. Cetinkaya, E. Yigit, C. Ozdemir, and A. A. Vertiy, “A study on millimeter-wave imaging of concealed objects: Application using back-projection algorithm,” *Progress In Electromagnetics Research*, Vol. 128, 457–477, 2012.

8. Fhager, A., S. K. Padhi, and J. Howard, "3D image reconstruction in microwave tomography using an efficient FDTD model," *IEEE Antennas and Wireless Propagation Letters*, Vol. 8, 1353–1356, 2009.
9. Golnabi, A. H., P. M. Meaney, and K. D. Paulsen, "Tomographic microwave imaging with incorporated prior spatial information," *IEEE Transactions on Microwave Theory and Techniques*, Vol. 61, No. 5, 2129–2136, May 2013.
10. Zhang, W. and A. Hoorfar, "Three-dimensional real-time through-the-wall radar imaging with diffraction tomographic algorithm," *IEEE Transactions on Geoscience and Remote Sensing*, Vol. 51, No. 7, 4155–4163, July 2013.
11. Ma, L., H.-Y. Wei, and M. Soleimani, "Planar magnetic induction tomography for 3D near subsurface imaging," *Progress In Electromagnetics Research*, Vol. 138, 65–82, 2013.
12. Smith, D., M. Leach, M. Elsdon, and S. J. Foti, "Indirect holographic techniques for determining antenna radiation characteristics and imaging aperture fields," *IEEE Antennas and Propagation Magazine*, Vol. 49, No. 1, 54–67, February 2007.
13. Leach, M. P., D. Smith, and S. P. Skobelev, "A modified holographic technique for planar near-field antenna measurements," *IEEE Transactions on Antennas and Propagation*, Vol. 56, No. 10, 3342–3345, October 2008.
14. Elsdon, M., O. Yurduseven, and D. Smith, "Early stage breast cancer detection using indirect microwave holography," *Progress In Electromagnetics Research*, Vol. 143, 405–419, 2013.
15. Yurduseven, O., D. Smith, B. Livingstone, V. Schejbal, and Z. You, "Investigations of resolution limits for indirect microwave holographic imaging," *International Journal of RF and Microwave Computer-Aided Engineering*, Vol. 23, No. 4, 410–416, July 2013.